Harmonic generation in silicon nitride ring resonators

Jacob S. Levy,[1,*] Mark A. Foster,[2] Alexander L. Gaeta,[2] and Michal Lipson[1,3]

[1]*School of Electrical and Computer Engineering, 428 Phillips Hall, Cornell University, Ithaca, NY 14853, USA*
[2]*School of Applied and Engineering Physics, 160 Clark Hall, Cornell University, Ithaca, NY 14853, USA*
[3]*Kavli Institute at Cornell for Nanoscale Science, Cornell University, Ithaca, NY 14853, USA*
[*]*jsl77@cornell.edu*

Abstract: We demonstrate second- and third-harmonic generation in a centrosymmetric CMOS-compatible material using ring resonators and integrated optical waveguides. The $\chi^{(2)}$ response is induced by using the nanoscale structure of the waveguide to break the bulk symmetry of silicon nitride (Si_3N_4) with the silicon dioxide (SiO_2) cladding. Using a high-*Q* ring resonator cavity to enhance the efficiency of the process, we detect the second-harmonic output in the visible wavelength range with milliwatt input powers at telecom wavelengths. We also observe third-harmonic generation from the intrinsic $\chi^{(3)}$ susceptibility of the silicon nitride. Phase matching of the harmonic processes occurs due to the near coincidence of indices of refraction of the fundamental mode at the pump frequency and the corresponding higher-order modes of the harmonic fields.

©2011 Optical Society of America

OCIS codes: (190.4400) Nonlinear optics, materials; (190.2620) Harmonic generation and mixing; (130.3120) Integrated optics devices.

References and links

1. M. A. Foster, A. C. Turner, J. E. Sharping, B. S. Schmidt, M. Lipson, and A. L. Gaeta, "Broad-band optical parametric gain on a silicon photonic chip," Nature **441**(7096), 960–963 (2006).
2. B. Corcoran, C. Monat, C. Grillet, D. J. Moss, B. J. Eggleton, T. P. White, L. O'Faolain, and T. F. Krauss, "Green light emission in silicon through slow-light enhanced third-harmonic generation in photonic-crystal waveguides," Nat. Photonics **3**(4), 206–210 (2009).
3. T. J. Kippenberg, S. M. Spillane, and K. J. Vahala, "Kerr-nonlinearity optical parametric oscillation in an ultrahigh-Q toroid microcavity," Phys. Rev. Lett. **93**(8), 083904 (2004).
4. T. Carmon and K. J. Vahala, "Visible continuous emission from a silica microphotonic device by third-harmonic generation," Nat. Phys. **3**(6), 430–435 (2007).
5. J. S. Levy, A. Gondarenko, M. A. Foster, A. C. Turner-Foster, A. L. Gaeta, and M. Lipson, "CMOS-compatible multiple-wavelength oscillator for on-chip optical interconnects," Nat. Photonics **4**(1), 37–40 (2010).
6. K. Ikeda, R. E. Saperstein, N. Alic, and Y. Fainman, "Thermal and Kerr nonlinear properties of plasma-deposited silicon nitride/ silicon dioxide waveguides," Opt. Express **16**(17), 12987–12994 (2008).
7. D. T. H. Tan, K. Ikeda, P. C. Sun, and Y. Fainman, "Group velocity dispersion and self phase modulation in silicon nitride waveguides," Appl. Phys. Lett. **96**(6), 061101–061103 (2010).
8. N. Bloembergen, R. K. Chang, S. S. Jha, and C. H. Lee, "Optical Second-Harmonic Generation in Reflection from Media with Inversion Symmetry," Phys. Rev. **174**(3), 813–822 (1968).
9. H. W. K. Tom, T. F. Heinz, and Y. R. Shen, "Second-Harmonic Reflection from Silicon Surfaces and Its Relation to Structural Symmetry," Phys. Rev. Lett. **51**(21), 1983–1986 (1983).
10. J. E. Sipe, D. J. Moss, and H. M. van Driel, "Phenomenological theory of optical second- and third-harmonic generation from cubic centrosymmetric crystals," Phys. Rev. B Condens. Matter **35**(3), 1129–1141 (1987).
11. Y. R. Shen, "Surface properties probed by second-harmonic and sum-frequency generation," Nature **337**(6207), 519–525 (1989).
12. S. Lettieri, S. D. Finizio, P. Maddalena, V. Ballarini, and F. Giorgis, "Second-harmonic generation in amorphous silicon nitride microcavities," Appl. Phys. Lett. **81**(25), 4706–4708 (2002).
13. S. Lettieri, F. Gesuele, P. Maddalena, M. Liscidini, L. C. Andreani, C. Ricciardi, V. Ballarini, and F. Giorgis, "Second-harmonic generation in hydrogenated amorphous-$Si_{1-x}N_x$ doubly resonant microcavities with periodic dielectric mirrors," Appl. Phys. Lett. **87**(19), 191110 (2005).
14. A. Gondarenko, J. S. Levy, and M. Lipson, "High confinement micron-scale silicon nitride high Q ring resonator," Opt. Express **17**(14), 11366–11370 (2009).
15. A. C. Turner, M. A. Foster, A. L. Gaeta, and M. Lipson, "Ultra-low power parametric frequency conversion in a silicon microring resonator," Opt. Express **16**(7), 4881–4887 (2008).

#146538 - $15.00 USD Received 28 Apr 2011; revised 22 May 2011; accepted 23 May 2011; published 26 May 2011

16. M. Ferrera, L. Razzari, D. Duchesne, R. Morandotti, Z. Yang, M. Liscidini, J. E. Sipe, S. Chu, B. E. Little, and D. J. Moss, "Low-power continuous-wave nonlinear optics in doped silica glass integrated waveguide structures," Nat. Photonics **2**(12), 737–740 (2008).
17. J. K. Ranka, R. S. Windeler, and A. J. Stentz, "Optical properties of high-delta air silica microstructure optical fibers," Opt. Lett. **25**(11), 796–798 (2000).
18. F. G. Omenetto, A. J. Taylor, M. D. Moores, J. Arriaga, J. C. Knight, W. J. Wadsworth, and P. S. J. Russell, "Simultaneous generation of spectrally distinct third harmonics in a photonic crystal fiber," Opt. Lett. **26**(15), 1158–1160 (2001).
19. A. Serpengüzel and S. Tanriseven, "Controlled photoluminescence in amorphous-silicon-nitride microcavities," Appl. Phys. Lett. **78**(10), 1388–1390 (2001).
20. M. Barth, N. Nusse, J. Stingl, B. Lochel, and O. Benson, "Emission properties of high-Q silicon nitride photonic crystal heterostructure cavities," Appl. Phys. Lett. **93**(2), 021112–021113 (2008).
21. V. R. Almeida, R. R. Panepucci, and M. Lipson, "Nanotaper for compact mode conversion," Opt. Lett. **28**(15), 1302–1304 (2003).
22. R. W. Boyd, *Nonlinear Optics*, 3rd ed. (Academic Press, San Diego, 2008).
23. S. F. Pereira, M. Xiao, H. J. Kimble, and J. L. Hall, "Generation of squeezed light by intracavity frequency doubling," Phys. Rev. A **38**(9), 4931–4934 (1988).
24. N. K. Hon, K. K. Tsia, D. R. Solli, and B. Jalali, "Periodically poled silicon," Appl. Phys. Lett. **94**(9), 091116–091113 (2009).

1. Introduction

The emerging field of silicon photonics seeks to unify the high bandwidth of optical communications with complementary metal-oxide-semiconductor (CMOS) microelectronic circuits. Many components have been demonstrated for on-chip optical communications, including those that utilize the nonlinear optical properties of silicon [1, 2], silicon dioxide [3, 4] and silicon nitride [5, 6]. Processes such as second harmonic (SH) generation, enabled by the second-order susceptibility, have not been developed in integrated optics since the bulk $\chi^{(2)}$ vanishes in these centrosymmetric materials. Generating the lowest-order nonlinearity enables a new array of CMOS-compatible optical devices capable of nonlinear functionalities such as electro-optic modulation, sum frequency up-conversion, and difference frequency generation.

Silicon nitride (Si_3N_4) is a centrosymmetric, CMOS compatible material shown to be useful for integrated optics and to possess interesting nonlinear properties [5–7]. In this study we induce a $\chi^{(2)}$ response utilizing the interface between two centrosymmetric materials, the Si_3N_4 core and the silicon dioxide (SiO_2) cladding. The waveguide interface breaks the bulk symmetry and a second-order nonlinear response can arise [8–11] from the asymmetric dipole potential formed at the surfaces. Previously, detecting the second harmonic wave from a reflected interface has been used for monitoring surface properties, even in centrosymmetric materials [9, 11], however no CMOS-compatible integrated devices have shown guided SH. Previous studies of SHG from the interface of thin film Bragg reflectors using various compositions of amorphous silicon nitride to form microcavities have shown resonant enhancement of the surface effect [12]. Additionally, it was shown that making the cavities doubly resonant, at both pump and harmonic wavelength, further increases the efficiency [13]. In this work we demonstrate for the first time in-plane and guided generation of the harmonic wave coupled from the doubly resonant cavity to an integrated waveguide, as opposed to simply observing the surface reflection effect with an out of plane configuration. Unlike previous work in the area, we are able to quantify the strength of the nonlinearity and conversion efficiency for our device; we generate significant power at the SH wavelengths compared to previous measurements which only report relative intensities with no absolute scale. Utilizing the intrinsic $\chi^{(3)}$ of Si_3N_4, we also measure the generated third-harmonic (TH) in the integrated cavities. Previously silica microtoroids on silicon [4] and silicon photonic crystals [2] have demonstrated TH, but this is the first demonstration to our knowledge of in-plane coupling of the generated light.

2. Design

We are able to effectively generate SH light by careful design of waveguide dimensions of a device based on recently demonstrated Si_3N_4 ring resonators with both high Q and high modal

#146538 - $15.00 USD Received 28 Apr 2011; revised 22 May 2011; accepted 23 May 2011; published 26 May 2011
(C) 2011 OSA

confinement [14]. Integrated ring resonators enhance the efficiency of nonlinear interactions [5, 15, 16] due to the large power build-up in the ring. We design silicon nitride ring resonators to be resonant at both fundamental and SH frequencies with the same fabrication process previously described [5, 14]. The ring resonator (Fig. 1(a)) used in this experiment has a radius of 116 µm and a coupling gap of 350 nm between the ring and the bus waveguide.

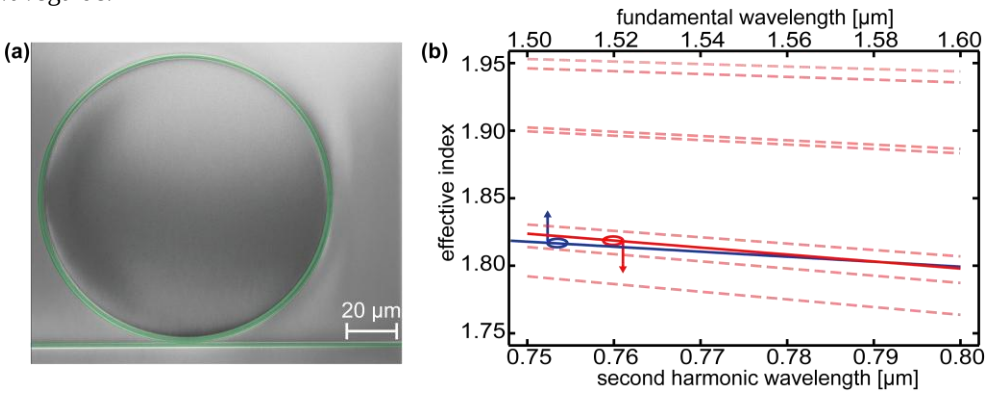

Fig. 1. Design of a silicon nitride ring resonator for second-harmonic generation. (a) A scanning electron micrograph image of a typical silicon-nitride ring microresonator. (b) The solid blue line represents the effective index of the fundamental quasi-TE mode at the IR pump as a function of wavelength for a waveguide with cross-sectional dimensions of 725x1500 nm. The dashed red lines represent the effective indices for modes of the corresponding SH wavelengths. The sixth-order mode of the SH (solid red) has a crossing with the blue line indicating a point of phase-matching.

Efficient SHG is possible by satisfying the phase-matching condition of matching the effective index of the fundamental waveguide mode in the IR to a higher order mode in the visible range. This method has previously been suggested for phase-matched third-harmonic generation in SiO_2, in both microtoroids [4] and microstructured fibers [17, 18]. In order to determine which mode is best phase-matched, we use a finite difference method mode solver to calculate the effective index for both the pump and SH frequencies. This calculation solves for the effective refractive index for a waveguide bending with a radius equivalent to that of the fabricated ring resonator. By solving for the effective index instead of a centrosymmetric cavity mode, we are able to fully take into account material dispersion and track the phase-matching for a continuum of wavelengths. Figure 1(b), shows a plot of the effective index against wavelength for the first 8 modes of the waveguide at the SH wavelength and the fundamental mode at the pump wavelength. Since the phase-matching condition is satisfied when the effective index at the pump and corresponding SH wavelengths are equal, crossing points between the blue and red lines are perfectly phase-matched for the corresponding wavelength pair and mode number. As the plot shows, we have a phase-matching point near our experimental pump wavelength with the 6th transverse waveguide mode at the SH wavelength.

3. Experimental results

3.1 Second-harmonic conversion

We measure the SH wavelength in the waveguide coupled to the resonator for input pump powers as low as 3 mW. A tunable diode laser is amplified using an erbium-doped fiber amplifier and coupled to the waveguide using a tapered lensed fiber. We use a polarization controller to launch light in the fundamental quasi-TE mode of the waveguide. The pump wavelength λ_P is tuned into the resonance of the ring cavity near 1554 nm and, with suitable power levels, we are able to observe generation of the second harmonic (Fig. 2(a)). We use a spectrometer to measure the wavelength of the visible emitted light. Figure 2(b) shows the output with the generated SH wavelength λ_{SH} measured to be 777.1 nm which, as expected, is

#146538 - $15.00 USD Received 28 Apr 2011; revised 22 May 2011; accepted 23 May 2011; published 26 May 2011
(C) 2011 OSA

$\lambda_P/2$. Since only the SH wavelength is detected, we conclude we are not generating broadband photoluminescence which has been previously described in silicon nitride [19, 20]. To measure the power of the SH, both the IR pump and the visible signal are collected into an optical spectrum analyzer (OSA). The powers measured by the OSA are corrected to the absolute power values coming out of the waveguide, taking into consideration the coupling efficiencies from the waveguide to the fiber and to the OSA for both pump and SH wavelengths, respectively. The OSA confirms the wavelength measurement for both the pump and SH. We observe a maximum conversion efficiency of −35 dB with 100 μW of SH generated for a pump of 315 mW. At increased pump powers, the ring's resonance experiences a thermal shift which prevents efficient coupling from the waveguide to the resonator.

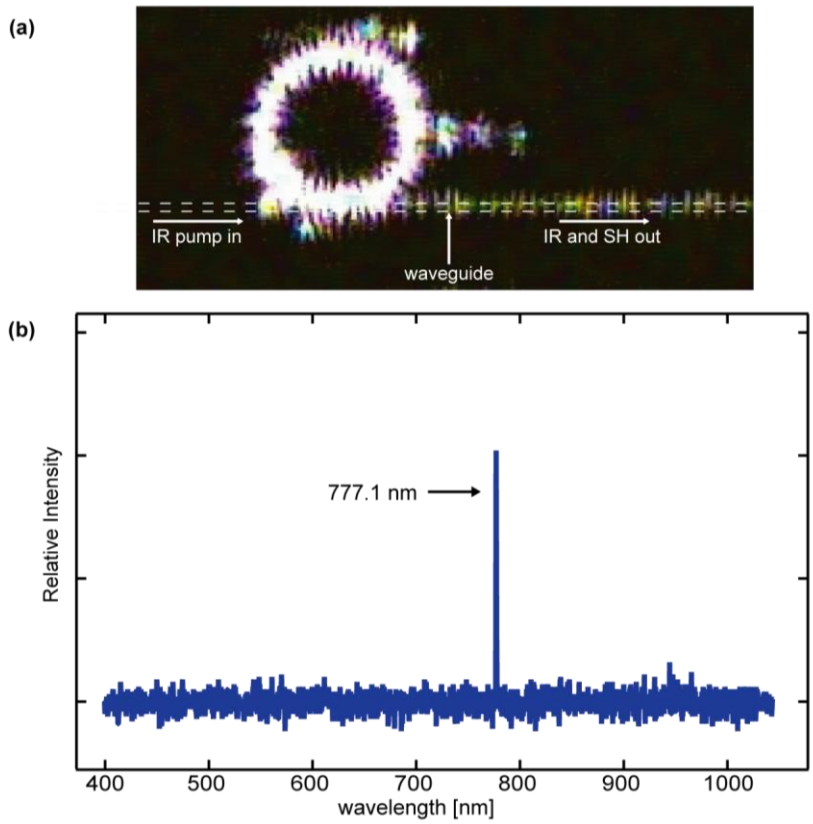

Fig. 2. The visible and spectral output from the generated SH light. (a). Top view visible CCD camera image of the microresonator generating red light. IR light, invisible to this camera, is launched from the left and couples into the ring. The power builds-up in the ring generating SH which couples back into the waveguide propagating out to the right. (b) The output from the waveguide, pumped at 1554.2 nm, is collected into an optical spectrometer. The visible emitted light occurs only at the expected SH wavelength

3.2 Modal profile image

The captured mode image of the waveguide output (Fig. 3) corresponds well to the simulated mode profile for the 6th order SH mode which optimizes the phase-matching condition. Since the ring and bus waveguide cross-sections are identical, we expect the same-order mode generated in the ring resonator to couple to the waveguide. To effectively image the mode, we polish away the nanotapers [21], used to increase coupling efficiency, at the output of the waveguide. We collect the output light with a high NA objective to focus the image on a CCD camera. There are three distinct lobes in the mode showing a good match with the simulated mode.

#146538 - $15.00 USD Received 28 Apr 2011; revised 22 May 2011; accepted 23 May 2011; published 26 May 2011
(C) 2011 OSA

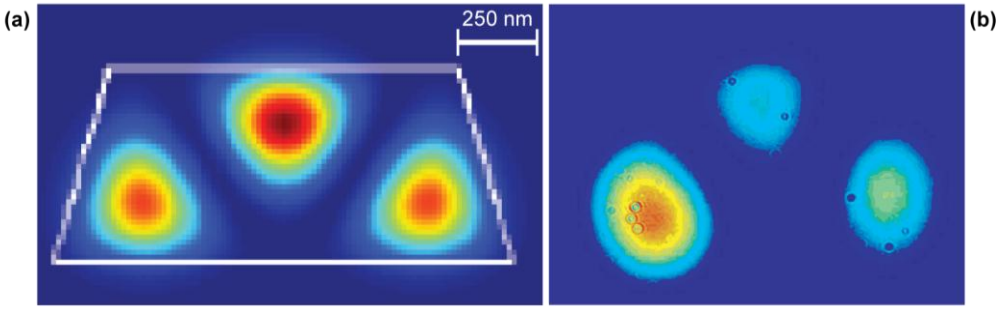

Fig. 3. Modal cross-section profiles for phase-mathched SH generation. (a) The simulated cross-section mode profile for the sixth-order mode of our waveguide at 777.1 nm. (b) The captured mode image of the visible emission from our waveguide showing good agreement with the simulated mode profile.

3.3 Third-harmonic generation

In addition to SH, we also observe third-harmonic generation in the ring resonators as shown in Fig. 4(a). The intrinsic $\chi^{(3)}$ nonlinearity of the silicon nitride induces the third order process in which three pump photons generate a single photon at the third-harmonic frequency. Efficient THG requires meeting the same phase-matching condition as SHG: the effective index of the pump must equal the effective index at the TH wavelength. By performing similar simulations as before we find the fundamental mode of the pump is closest in refractive index to the 18th order mode at the third-harmonic wavelength.

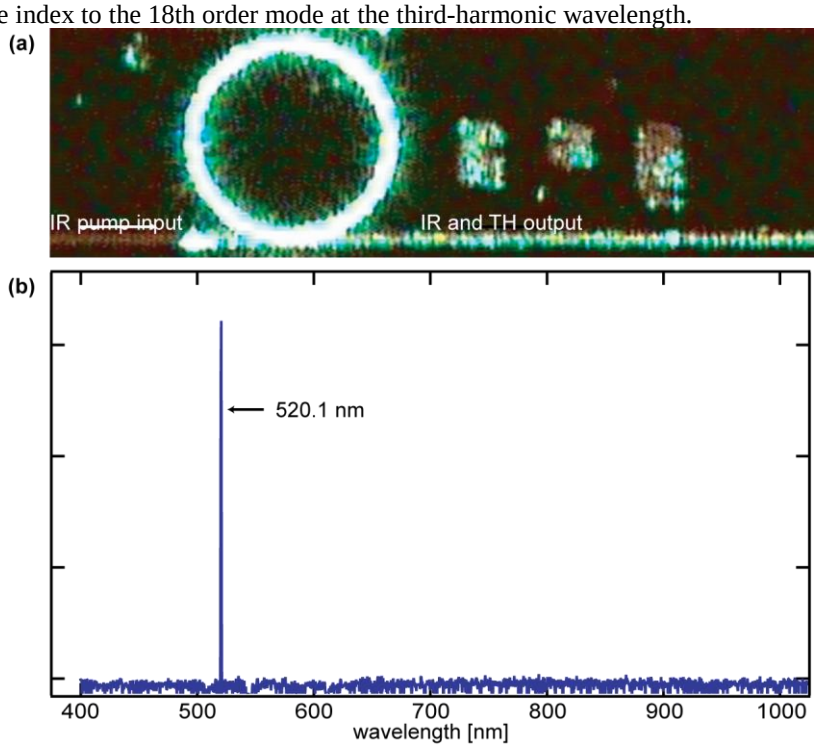

Fig. 4. Third-harmonic generation in silicon nitride resonators. (a) Top view CCD image of waveguide coupled ring resonator generating visible TH from an IR pump tuned to the cavity resonance. (b) Spectrometer output from the waveguide shown in (a). The monochromatic response confirms the wavelength and that THG is occurring.

By pumping at a resonance near 1560 nm, we generate the TH and measure the light to be exactly one third of the pump wavelength (Fig. 4). We are able to measure picowatts of output power with for the same pump strength as used to generate SH light. This is on the same order

#146538 - $15.00 USD Received 28 Apr 2011; revised 22 May 2011; accepted 23 May 2011; published 26 May 2011
(C) 2011 OSA

as shown in a silicon photonic crystal [2], but here light is coupled and guided in the bus waveguide as opposed to out of plane emission.

4. Analysis

We calculate the effective $\chi^{(2)}$ to be as large as 4 x 10^{-14} m/V from the conversion efficiency observed in the ring. For SHG with an undepleted pump, the expected signal power may be calculated for a given pump intensity and propagation distance by solving the coupled amplitude equations [22]. Since we are using a resonator, the intensity of the pump and SH are increased by the respective cavity enhancement effects of the ring. In order to accurately model the nonlinear susceptibility, we take into account the finesse of the cavity, the simulated modal field overlap and phase-mismatch, and the radius of the ring. The power P_{sh} for second harmonic wave is then given by:

$$P_{sh} = \frac{C_{sh} C_p^2 (\omega_p \chi^{(2)} L P_p)^2}{8 n_p^2 n_{sh} c^3 \epsilon_0 A_p^2} A_{sh} \sin c^2(\Delta k L/2)\ f(A_p, A_{sh}),$$
$$C_i = \frac{P_{circ}}{P_{in}} = \left| \frac{j\kappa_i \exp(-\alpha_i L/2)}{\exp(jk_i L) - \tau_i \exp(-\alpha_i L/2)} \right|^2 \quad (1)$$

where ω_p is the pump frequency, ε_0 is the permittivity of free space, c is the speed of light in vacuum, n_i is the effective index for the modes, A_i is the mode area, Δk is the phase mismatch, L is the ring circumference and P_p is the pump power in the waveguide. The modal overlap integral between the fundamental and second-harmonic fields is accounted for by the function $f(A_p, A_{sh})$. C_i takes into account the circulating power in the ring [15] where κ and τ represent the coupling parameters from the waveguide to the ring, α is the propagation loss in the ring and k_i is the wavenumber. We can directly measure C_p from the transmission spectrum of the pump resonance and calculate this to be approximately 156. For the SH resonance we are unable to directly characterize the intrinsic and coupling Q's. We estimate that C_{sh} is at most C_p and at least unity. From this approximation we come up with a range of potential values for the effective $\chi^{(2)}$ 3 x 10^{-15} to 4 x 10^{-14} m/V. We believe the actual enhancement at the SH wavelength is closer to unity than C_p and therefore the effective $\chi^{(2)}$ to be on the larger side of the approximation range. From Eq. (1), we see that the SH wave has a quadratic dependence on the pump power and nonlinear susceptibility $\chi^{(2)}$. In order to clearly demonstrate the theoretical square dependence of the SH process, we plot the dropped pump power against the generated SH on a log-log scale (Fig. 5) and calculate a best fit slope of 1.9745 ± 0.0225. From the measured output power values we estimate our induced $\chi^{(2)}$. The integrated high finesse resonator in silicon nitride increases the efficiency of the SHG significantly when the pump and SH are both resonant.

#146538 - $15.00 USD Received 28 Apr 2011; revised 22 May 2011; accepted 23 May 2011; published 26 May 2011
(C) 2011 OSA

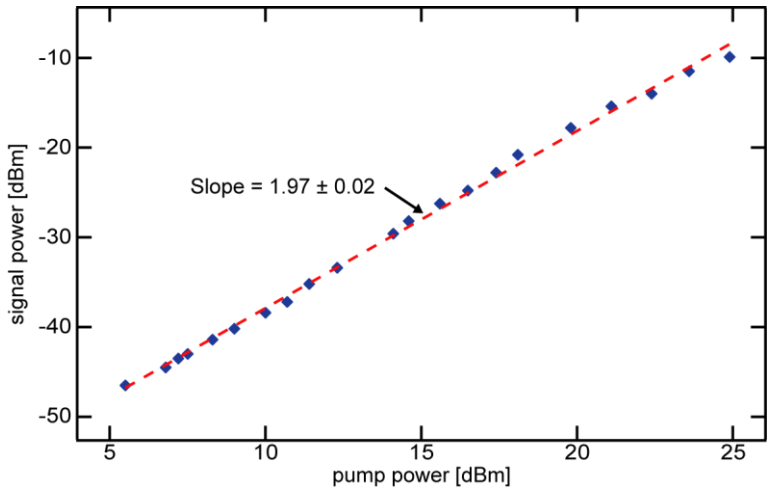

Fig. 5. The power dependence of generated SH coupled out versus pump power dropped to the ring. The red-dashed line with slope near 2 on the log-log plot represents the best fit line of the experimental data and is very close to the theoretical square prediction.

The $\chi^{(3)}$ response in silicon nitride has been previously examined [5–7] by quantifying the nonlinear refractive index, n_2, through the Kerr-shift, self-phase modulation and four-wave mixing respectively. Like previous work involving SiO_2 resonators [4], we expect to see THG with high enough circulating powers and phase-matching to higher order modes from the bulk nonlinearity as opposed to an enhanced surface effect with the SHG. From the spectrometer measurements taken to confirm the wavelength of the harmonic, we can measure the collected photons over a specified integration time. From this data we calculate the collected power to be on the order of picowatts with a maximum input power of 120 mW dropped into the ring. Given the circulating power in the resonator, the nonlinearity of the material and the cubic dependence of the third-harmonic power on the pump intensity, we expect much stronger conversion efficiencies. We believe that imperfect phase-matching and the weak spatial overlap between the fundamental and third-harmonic modes may account for the weaker than expected third harmonic. Therefore, our estimation of the effective $\chi^{(2)}$ could be a lower bound since we assume ideal phase-matching, as suggested by our simulations, in this approximation.

5. Conclusions

Our demonstration of guided on-chip visible light generation opens the available spectrum for Si-based devices from the IR to the visible, increasing bandwidth and enabling potential integration of silicon photodetectors to on-chip optical networks. We have demonstrated an integrated coupling of both the second and third harmonics from a cavity to a waveguide for the first time on a silicon platform. Additionally, the doubly resonant SH generation presented here could produce squeezed states [23] of both the pump and SH frequencies for quantum optics studies. Finally, the induced second-order nonlinearity could be used for difference frequency generation to combine two near infrared pumps to generate a mid-infrared source [24].

Acknowledgements

The authors would like to acknowledge DARPA for supporting this work under the MTO POPS Program. This work was performed in part at the Cornell NanoScale Facility, a member of the National Nanotechnology Infrastructure Network, which is supported by the National Science Foundation (Grant ECS-0335765).

#146538 - $15.00 USD Received 28 Apr 2011; revised 22 May 2011; accepted 23 May 2011; published 26 May 2011
(C) 2011 OSA